JCTC Journal of Chemical Theory and Computation

Article

pubs.acs.org/JCTC

Solute–Solvent Charge-Transfer Excitations and Optical Absorption of Hydrated Hydroxide from Time-Dependent Density-Functional Theory

Daniel Opalka* and Michiel Sprik

Department of Chemistry, University of Cambridge, Cambridge CB2 1EW, United Kingdom

ABSTRACT: The electronic structure of simple hydrated ions represents one of the most challenging problems in electronic-structure theory. Spectroscopic experiments identified the lowest excited state of the solvated hydroxide as a charge-transfer-to-solvent (CTTS) state. In the present work we report computations of the absorption spectrum of the solvated hydroxide ion, treating both solvent and solute strictly at the same level of theory. The average absorption spectrum up to 25 eV has been computed for samples taken from periodic ab initio molecular dynamics simulations. The experimentally observed CTTS state near the onset of the absorption threshold has been analyzed at the generalized-gradient approximation (GGA) and with a hybrid density-functional. Based on results for the lowest excitation energies computed with the HSE hybrid functional and a Davidson diagonalization scheme, the CTTS transition has been found 0.6 eV below the first absorption band of liquid water. The transfer of an electron to the solvent can be assigned to an excitation from the solute 2pπ orbitals, which are subject to a small energetic splitting due to the asymmetric solvent environment, to the significantly delocalized lowest unoccupied orbital of the solvent. The distribution of the centers of the excited state shows that CTTS along the OH^- axis of the hydroxide ion is avoided. Furthermore, our simulations indicate that the systematic error arising in the calculated spectrum at the GGA originates from a poor description of the valence band energies in the solution.

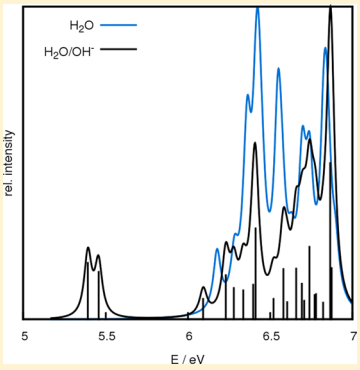

1. INTRODUCTION

The electronic structure of liquid water and hydrated ions has received much attention in theoretical and experimental research. Experiments revealed that hydrated halide and hydroxide ions can be excited into charge-transfer-to-solvent (CTTS) states by absorption of photons in the ultraviolet (UV) spectral range. As the excited electronic state relaxes, a substantial yield of hydrated electrons is produced. Both hydrated electrons and hydroxyl radicals are among the highest reactive species of biological relevance and one of the origins for radiation damage to living organisms.[1,2]

Important experimental techniques to analyze the electronic band structure of liquid water are optical absorption spectroscopy[3−5] and, more recently, liquid-microjet photoemission spectroscopy.[6] Photoemission spectroscopy on the solvated hydroxide probes the positions of the occupied molecular orbitals (MOs) of the solute and the valence band of the solvent relative to vacuum. Optical spectroscopy, on the other hand, provides information about the structure of the conduction band and possibly unoccupied electronic states of the solute as well as interactions between the electronic structure of solute and solvent. Moreover, spectroscopic techniques in combination with molecular dynamics simulations and electronic-structure calculations significantly contributed to our understanding of the solvation structure of hydrated OH^-.[7]

One of the many unusual properties of water is the blue shift of the ionization potential and UV absorption energies in bulk water compared to isolated molecules in the gas phase. The electronic transitions observed in the UV absorption spectrum of water are often interpreted as a number of Rydberg series, primarily from the $^1b_1$ highest occupied molecular orbital (HOMO). The Rydberg progressions converge to the ionization potential of the respective ionic state,[3−5,8] and the blue shift has been interpreted as destabilization of the molecular Rydberg states due to the solvent molecules. A similar blue shift has been observed for dissolved ions, both for the vertical ionization potential (IP) and optical excitations.

Winter et al. determined the vertical ionization energy of the solvated hydroxide ion at 9.2 eV using liquid microjet photoemission spectroscopy, 0.7 eV lower than the extrapolated ionization threshold of liquid water.[9] This represents a significant blue shift compared to the gas phase ionization potential of 1.83 eV.[10,11] Fox and co-workers systematically investigated the UV absorption spectra of various solvated halide ions and aqueous hydroxide.[12] The CTTS transition in liquid water at 298 K was found at 6.6 eV and strongly dependent on the solvent.[12,13] The adiabatic ionization potential of the OH^-/OH radical pair has been determined as 6.1 eV from published experimental data.[14] This agrees very well with the experimentally observed electron detachment after photoexcitation. Hence excitation to the CTTS electronic

Received: April 3, 2014
Published: May 14, 2014

   dx.doi.org/10.1021/ct5002889 | J. Chem. Theory Comput. 2014, 10, 2465−2470

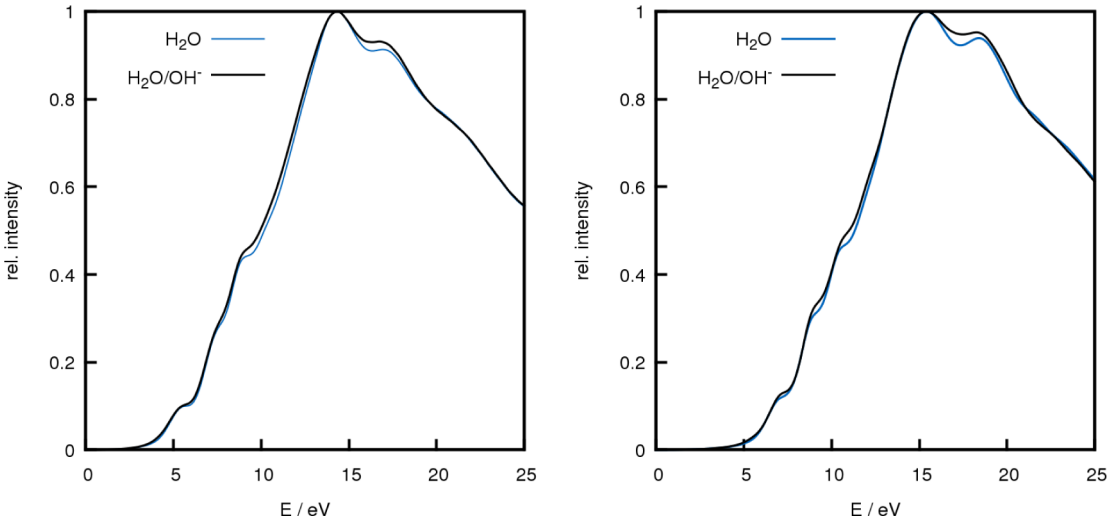

Figure 1. Averaged absorption spectra of a periodic 31 H_2O/OH^- system computed with time-dependent density-functional perturbation theory at the generalized-gradient approximation (left) and with a hybrid functional (right). For comparison also the computed absorption spectrum of a pure water system is shown. All spectra have been convoluted with a Lorentz function.

state proved to be very useful for the generation and analysis of hydrated electrons and hydroxyl radicals.[15−17]

The CTTS states of halide ions and hydroxide are often considered similar in the literature. Despite some similarities regarding their vertical IP and density of states, however, a number of fundamental differences exist. As a diatomic system, the hydroxide ion can store vibrational energy and responds to electronic excitation by a change in geometry. "Hot" hydroxide has been observed by femtosecond spectroscopy on the CTTS state which contributed to the relaxation dynamics after photoexcitation.[15−17] Furthermore, the OH^- ion is tightly integrated into the hydrogen bond network, both with acceptor bonds and a weak donor bond.[7] Halide ions, on the other hand, form hydrogen bonds with the surrounding water molecules and polarize the solvent molecules. Experimentally it has also been found that halide ions tend to reside at the water surface, while OH^- ions show no preference compared to the bulk.[18]

From a theoretical perspective the description of optical properties of liquid water and solvated ions turned out to be very difficult but is indispensable to understand the microscopic mechanisms of solute−solvent interactions and electron-transfer reactions. Previous work mostly focused on relatively small clusters in the gas phase.[19−21] This represents a serious limitation for the description of the solvent environment and the usually strongly delocalized CTTS states which lead to the ejection of an electron into the solvent. As is well-known, density functional theory (DFT) in the local-density or generalized-gradient approximation does not account for the screening of long-range electronic Coulomb interactions and suffers from the self-interaction error. Recent theoretical work on the electronic properties of liquid water has focused on corrections of the self-interaction error using many-body perturbation theory within the GW and BSE approximations.[22−25] An alternative approach to improve the electronic exchange-correlation energy is to combine DFT with the (exact) exchange energy of the Hartree−Fock method, building on the success of hybrid functionals in the description of band gaps in molecular systems.[26] Bernasconi computed the absorption spectrum of liquid water using TDDFT with hybrid- and accurate orbital dependent exchange-correlation functionals and the adiabatic local density approximation kernel.[27] The results indicate that accurate initial orbitals may improve the energy levels of the electronic excitations.

Recently developed functionals also account for screening effects and may improve the description of electronic properties while avoiding the complexity of correlated electronic-structure methods. In this work we use the Heyd-Scuseria-Ernzerhof functional to compute the UV absorption spectrum of the hydrated OH^- ion with an iterative Lanczos and a Davidson diagonalization algorithm based on time-dependent density functional perturbation theory.[28,29]

2. COMPUTATIONAL DETAILS

The electronic spectrum of a solute in liquid water depends on the instantaneous molecular structure, in particular the solvation shell, when the spectrum is recorded. In computer simulations this effect can be modeled by taking the average over a representative number of configurations. We used trajectories from ab initio molecular dynamics simulations to generate a set of molecular geometries which have been validated by calculation of the density of states (DOS) and structural properties such as radial distribution functions. The molecular dynamics simulations have been performed with the Quantum Espresso software distribution,[30] and all calculations were carried out at the Γ-point.

The electronic structure calculations to obtain the molecular forces were performed with the generalized gradient approximation (GGA) employing the Becke−Lee−Yang−Parr (BLYP) exchange-correlation functional.[31,32] The core−electrons have been described by norm-conserving (Troullier-Martins) pseudopotentials, and the cutoff energy for the plane-wave basis was set to 70 Ry. In our simulations we have used a cubic cell with periodic boundary conditions and the experimental volume of 32 water molecules at a temperature of 330 °C. For the simulation one hydrogen nucleus had been removed to create a single dissolved hydroxide ion. It has been shown that the structure of liquid water determined with the BLYP functional at temperature a little higher than room temperature is in better agreement with experimental data.[33] The 31 H_2O molecules and the OH^- ion have been propagated as an NVT ensemble for more than 20 ps after an initial equilibration period of 2 ps. Previous work of Costanzo et al.

shows that the effect of a localized excess charge is negligible for the computation of solvation energies and acidity constants.[34] Based on these results, we have not applied any additional corrections to screen the interactions of the excess charge in the periodic simulation cell.

Snapshots every 500 fs were taken from the trajectory and used for the computation of the absorption spectra. The calculations of the full absorption spectrum were performed with time-dependent density-functional perturbation theory (TDDFPT) and a Lanczos iteration scheme, developed and implemented in QE by Malcioglu et al.[28] Absorption spectra have been computed for 40 snapshots using the GGA and for 6 geometries with a hybrid exchange-correlation functional. In the electronic structure calculations for the TDDFPT spectra the electron-density was described by a plane-wave basis set and the Perdew–Burke–Ernzerhof (PBE)[35,36] and the Heyd-Scuseria-Ernzerhof (HSE)[37,38] exchange-correlation functional at the GGA and hybrid level of theory, respectively. Both the hybrid and the GGA calculations were performed with a pseudopotential obtained for the PBE functional. Due to the high computational cost the number of Lanczos iterations has been limited to 5000 for the GGA and 2000 for the hybrid-functional calculations in all three polarization directions. The Lanczos coefficients have been extrapolated up to 10000 iterations, and the average over all spectra from different snapshots of the trajectories was taken. We applied a Lorentzian broadening of 0.5 eV to all computed spectra to simulate the finite line width. Additionally, high resolution spectra for the lowest 20 electronic transitions have been computed by a Davidson diagonalization method recently implemented in the QE software distribution.[29]

3. RESULTS AND DISCUSSION

The UV absorption spectrum of a diluted aqueous solution of hydroxide ions at low resolution is dominated by the absorption bands of liquid water. The absorption spectrum of liquid water below the ionization threshold around 9.9 eV is characterized by three broad absorptions bands. Mota and co-workers have assigned the first three transitions to excitations from the electronic $\tilde{X}^1A_1$ ground state to the $\tilde{A}^1B_1$, $\tilde{B}^1A_1$, and $\tilde{C}^1B_1$ state, respectively, based on experimental data.[5] Figure 1 shows the UV absorption spectrum computed with the GGA and the HSE hybrid functional. As observed in experiment, the computed spectra show several broad and overlapping absorption bands. Three absorption bands can be identified in the energy range up to the ionization threshold. These valence excitations originate from the solvent molecules, and, in a molecular picture, the first electronic transition occurs by promotion of an electron from the $^1b_1$ HOMO to an empty $4a_1$ molecular orbital. The continuum between the first band up to the ionization threshold has been assigned to transitions leading to homolytic bond cleavage, producing an OH and a H radical.[5] In the GGA spectrum, the first main absorption bands up to the ionization threshold appear approximately at 5.6 eV, 7.5 eV, and 8.6 eV. Compared with the experimental water spectrum with the first absorption band at 7.4 eV, the GGA fails to reproduce the optical gap of water and is significantly red-shifted. Also no CTTS transition from the hydroxide ion to the solvent can be determined from the low-resolution spectrum. The spectrum on the rhs in Figure 1 has been computed with the HSE hybrid functional and appears at approximately 1.8 eV higher energy with respect to the GGA in significantly better agreement with the experiment. Approximate positions of the centers of the absorption bands determined from Figure 1 and experimental data from the literature are summarized in Table 1. Overall, the HSE low resolution spectrum exhibits very similar features as the spectrum computed at the GGA level.

Table 1. Approximate Positions of the Absorption Bands of a 31 H_2O/OH^- System from Time-Dependent Density-Functional Perturbation Theory[a]

	CTTS	$\tilde{A}^1B_1$	$\tilde{B}^1A_1$	$\tilde{C}^1B_1$
PBE	4.1	5.6	7.5	8.6
HSE	5.4	7.0	9.0	10.5
experiment[5,12]	6.6	7.4	9.7	10.0

[a]The centers of the experimentally determined absorption bands of liquid water are provided for comparison. All values in the table are given in eV.

A more detailed picture emerges from the onset of the computed absorption spectrum in the energy range of the expected CTTS transition. Figure 2 compares the computed absorption spectra of a pure water reference system and the hydroxide solution. In the averaged GGA spectrum, shown on the lhs of Figure 2, the CTTS state is covered by the pre-edge absorption band of liquid water centered around 5.4 eV. This band is most likely an artifact of the GGA and was also found in recent work on liquid water by Bernasconi[27] but is reduced by correlated methods (e.g., GW, BSE) or the use of accurate ground-state orbitals.[27] The HSE spectrum of pure water, shown on the rhs of Figure 2, lacks the pre-edge feature of the GGA spectra. However, the HSE spectrum of the aqueous hydroxide exhibits an extended onset into the low energy region which is absent in the spectrum of the pure solvent. A similar low-energy tail has been observed in the experimental photoemission spectrum of aqueous NaOH solution corresponding to ionization from the HOMO of OH^-. The experimental position of the nearly degenerate $2p\pi$ HOMO of solvated hydroxide was determined at 0.7 eV above the valence band of liquid water. Thus, in the UV spectrum, the low-energy band can be assigned to the CTTS state from the hydroxide ion to the solvent and lies approximately 0.6–0.7 eV below the absorption threshold of water—in good agreement with the experiment. The averaged onset in Figure 2, however, also indicates variations in the position of the CTTS band as the solvation shell fluctuates. This is also reflected in the large fwhm of 1.15 eV in the experimental photoemission spectrum.[39] Our simulations therefore suggest that the excitation of OH^- through absorption of a UV photon initiates an electronic transition directly to the conduction band of liquid water.

In order to further analyze the optical CTTS excitation we have computed the lowest 20 transitions with a Davidson diagonalization scheme.[29] This allows a direct assignment of the electronic CTTS transitions in terms of molecular orbitals. In an isolated OH^- ion, the $2p\pi$ HOMOs are exactly degenerate. Thus, the CTTS is characterized by two energetically close transitions originating from an electron in the HOMO and the second HOMO of the solute in its electronic ground state, which is excited to the considerably delocalized LUMO of bulk water. Since the CTTS in the GGA lies very close to the electronic transitions among the solvent molecules, we have computed the excitation energy as the average of the lowest two eigenvalues obtained by the Davidson algorithm. The average absorption frequency from 40 snapshots of the MD

dx.doi.org/10.1021/ct5002889 | J. Chem. Theory Comput. 2014, 10, 2465–2470

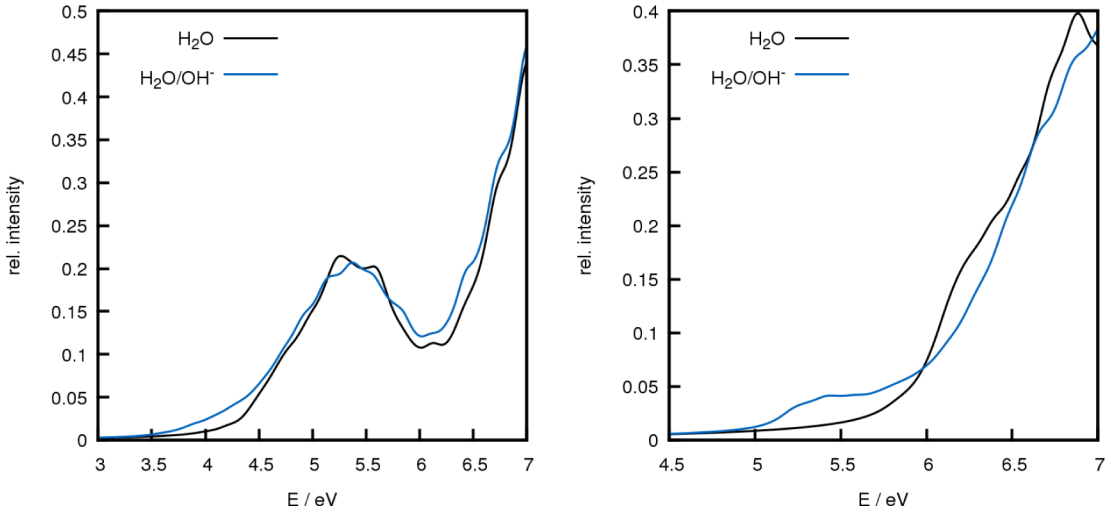

Figure 2. Onset of the simulated absorption spectrum computed with time-dependent density-functional perturbation theory. Left: GGA spectrum for a pure water and a 31 H_2O/OH^- system convoluted with a Lorentz function and averaged over 40 snapshots. Right: HSE spectrum of a 31 H_2O/OH^- system convoluted and averaged over six samples.

trajectory has been found at 4.1 eV very close the average value of the first transition between solvent molecules at 4.4 eV. This error is a consequence of the well-known delocalization error of the GGA in the description of the localized solute orbitals. Figure 3 displays the onset of the absorption spectrum for a single snapshot of the MD trajectory, computed at the hybrid-DFT level. The spectra exhibit two energetically close transitions at approximately 5.4−5.5 eV corresponding to the CTTS transition. A potential source of error in the HSE calculations is the neglect of long-range Hartree−Fock (HF) exchange. To examine the effect of long-range contributions, Figure 3 also shows the five lowest transitions computed with the PBE0 density functional. Both functionals produce very similar spectra for the first electronic transitions, and these results indicate that screening of the HF exchange is a valid approximation for periodic systems as considered in the present work.

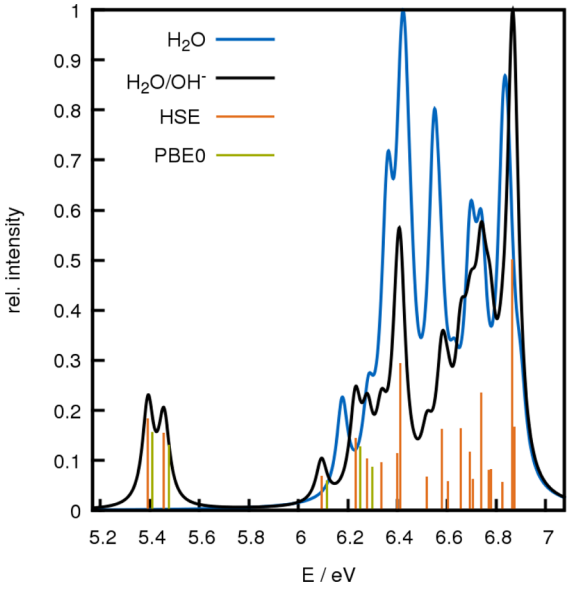

Figure 3. Convoluted and high resolution spectrum of a 31 H_2O/OH^- (black and orange) compared to pure water (blue). The 20 lowest electronic transitions are shown for both systems, illustrating the CTTS excitation from the 2pπ orbitals of the hydroxide ion around 5.4 eV. Due to the inhomogeneous solvation structure the degeneracy of the two transition is lifted.

Figure 4 shows the two Kohn−Sham HOMOs for the snapshot which has been used to compute the spectrum in Figure 3. Both orbitals show the expected characteristics of the 2pπ orbitals present in an isolated OH^- ion. Hence we can assume that the Kohn−Sham orbitals provide a realistic description of the two lowest electronic transition. Contrary to hydroxide in the gas phase, hydrogen bonds with the surrounding water molecules and, more general, solvation effects lift the degeneracy of the two HOMOs and split the absorption frequencies depending on the instantaneous hydration structure. According to our results this energetic difference between the HOMO and the second HOMO is small as already pointed out by Winter et al. in their analysis of a liquid-microjet photoemission experiment.[39]

As the solvation shell fluctuates the position of the CTTS band changes, and for an averaged spectrum only a smeared feature can be observed in the simulated absorption spectrum (Figure 2). An important aspect for the characterization of the CTTS is its dependence on the orientation of the principal axis of the hydroxide ion. We have addressed this question by computing the center of the LUMO of a set of geometries extracted from the MD trajectory and correlating its position with the OH-bond axis of the solvated OH^-. In Figure 5 an example of a LUMO orbital is shown. The O and H atom of the hydroxide ion are represented by a red and white sphere, respectively, while the solvent molecules are illustrated with a stick representation.

The rhs in Figure 5 illustrates the distribution of the LUMO centers with respect to the orientation of the solute where we have adopted the nearest image convention and the four closest images of the LUMO centers are shown. Furthermore, the nuclear coordinates of OH^- and the coordinates of LUMO centers have been rotated into the drawing plane to simplify the comparison. From Figure 5 it can be concluded that there exists a clear preference toward charge transfer with a perpendicular component with respect to the molecular axis. There are no CTTS excitation directed along the OH bond observed, and

dx.doi.org/10.1021/ct5002889 | J. Chem. Theory Comput. 2014, 10, 2465−2470

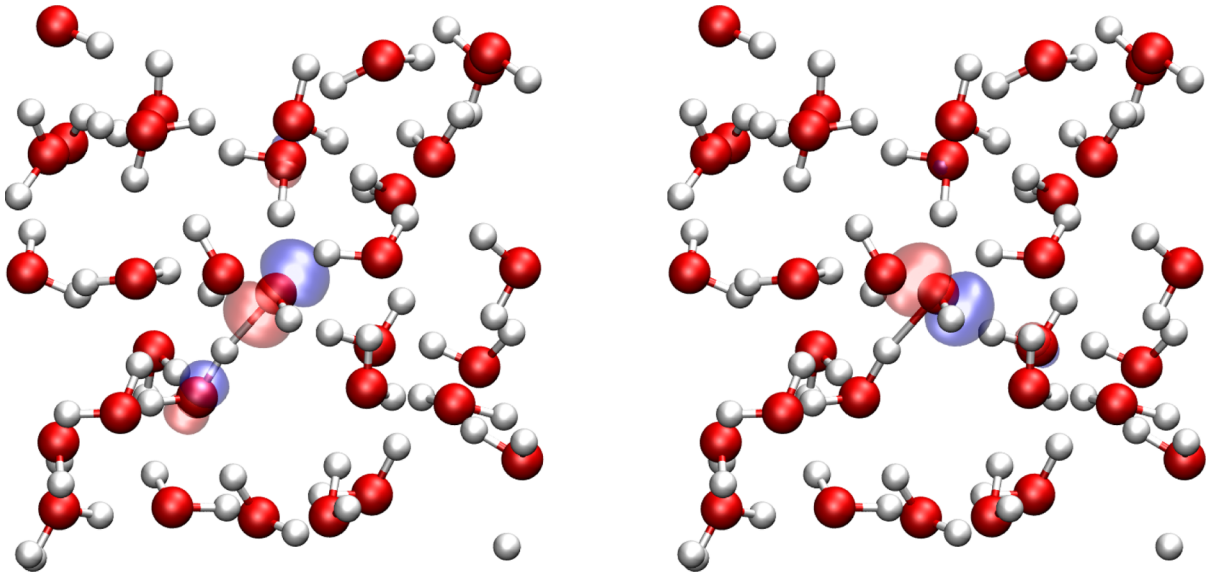

Figure 4. HOMO (left) and second HOMO (right) of a solvated hydroxide ion in a simulation box with 31 water molecules. The Kohn–Sham orbitals obtained with the HSE density functional are shown. Electrons excited from these orbitals are subject to a CTTS transition into the LUMO of bulk water.

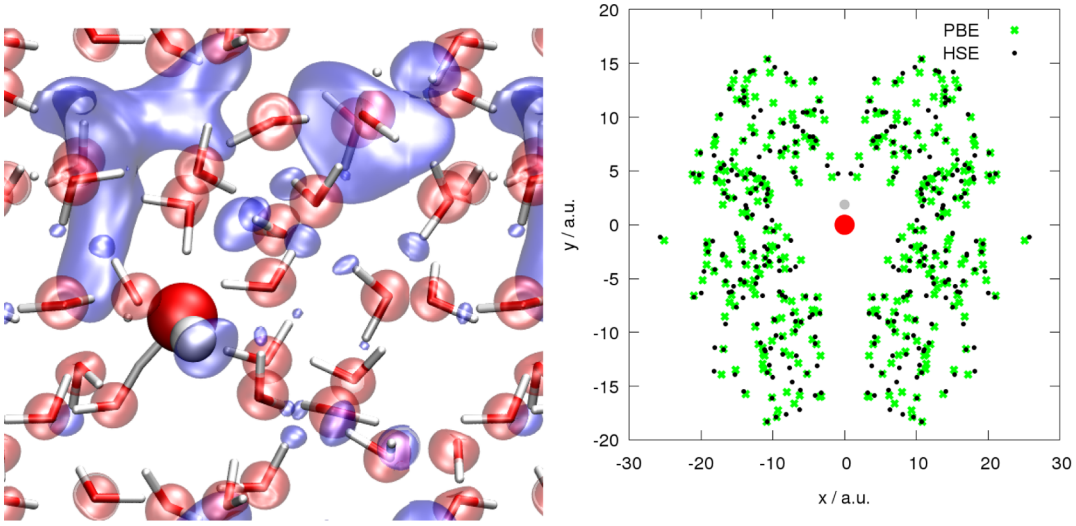

Figure 5. Left: LUMO of the solvated hydroxide ion computed at the HSE level of DFT from a snapshot of a MD trajectory. Right: Distribution of the centers of the LUMO for 40 different samples including four periodic images for each geometry. The vectors connecting the O atom in the OH^- ion and the LUMO centers have been rotated into the drawing plane, and two equivalent images are shown for each data point. Due to symmetry there is no preferred orientation around the OH axis in the hydroxide ion.

the data points tend to accumulate near the boundary of the periodic simulation cell. The long average distance of the CTTS state from the solute indicates that microsolvation studies on small clusters can not describe the CTTS or the formation of solvated electrons through photoexcitation.

4. SUMMARY

The UV absorption spectrum of the hydrated hydroxide has been computed for a periodic system, sampled from an ab initio MD trajectory. The main features of the experimental spectrum are reproduced by the low-resolution linear-response spectra, although the GGA leads to a substantial red-shift. The averaged GGA spectrum shows a characteristic absorption band around 5.4 eV which originates from bulk water and overlaps with the CTTS band. A similar feature has been observed in previous work on pure water and acetone–water systems.[27,40,41] From the onset of the HSE spectrum the CTTS electronic transitions have been assigned. In particular, the high resolution spectrum in Figure 3 illustrates the transitions from the 2pπ orbitals of the solute which are absent in the water reference spectrum. The high-resolution spectrum shows a small solvent shift due to the asymmetric solvent shell which lifts the degeneracy. No significant differences between calculations with the screened hybrid HSE and global hybrid PBE0 density functional were observed.

However, our calculations do not support the interpretation of Bernasconi[27] that the error in the low-energy region of the GGA can be attributed to a poor description of the unoccupied states of water. In order to analyze the CTTS from the HOMO of the solute to the LUMO of bulk water, we computed the centers of the significantly delocalized LUMO relative to the hydroxide ion for a set of geometries. The data shows

dx.doi.org/10.1021/ct5002889 | J. Chem. Theory Comput. 2014, 10, 2465–2470

preference for the LUMO to be located close to the boundary of the (periodic) simulation box, avoiding axial alignment with the OH-bond of the solute. No significant difference was observed between the GGA and the HSE LUMOs. Additionally, the energy difference in the HSE spectrum between the CTTS absorption and the first absorption band due to the solvent have been found to be the same as the experimental gap between the OH^- HOMO and valence band maximum of bulk water. The similar distribution of the LUMO centers in combination with the correct absorption onset of the HSE spectrum indicates that the error originating in the GGA primarily affects energy levels of the occupied orbitals.

AUTHOR INFORMATION

Corresponding Author

*E-mail: do293@cam.ac.uk.

Notes

The authors declare no competing financial interest.

ACKNOWLEDGMENTS

This work was supported by a research fellowship of the Deutsche Forschungsgemeinschaft for DO. Computing resources provided by the Leibniz Rechenzentrum of the Bavarian Academy of Sciences are gratefully acknowledged.

REFERENCES

(1) von Sonntag, C. In *Free-Radical-Induced DNA Damage and Its Repair*; Schreck, S., Ed.; Springer: Heidelberg, 2006.
(2) Halliwell, B.; Gutteridge, J. M. C. *Free Radicals in Biology and Medicine*, 4th ed.; Oxford University Press: New York, 2007.
(3) Price, W. C. *J. Chem. Phys.* **1936**, *4*, 147−153.
(4) Gürtler, P.; Saile, V.; Koch, E. E. *Chem. Phys. Lett.* **1977**, *51*, 386−391.
(5) Mota, R.; Parafita, R.; Giuliani, A.; Hubin-Franskin, M.-J.; Lourenço, J.; Garcia, G.; Hoffmann, S.; Mason, N.; Ribeiro, P.; Raposo, M.; Limão-Vieira, P. *Chem. Phys. Lett.* **2005**, *416*, 152−159.
(6) Winter, B.; Weber, R.; Widdra, W.; Dittmar, M.; Faubel, M.; Hertel, I. V. *J. Phys. Chem. A* **2004**, *108*, 2625−2632.
(7) Marx, D.; Chandra, A.; Tuckerman, M. E. *Chem. Rev.* **2010**, *110*, 2174−2216.
(8) Rubio, M.; Serrano-Andrés, L.; Merchán, M. *J. Chem. Phys.* **2008**, *128*, 104305.
(9) Winter, B.; Faubel, M. *Chem. Rev.* **2006**, *106*, 1176−1211.
(10) Schulz, P. A.; Mead, R. D.; Jones, P. L.; Lineberger, W. C. *J. Chem. Phys.* **1982**, *77*, 1153−1165.
(11) Smith, J. R.; Kim, J. B.; Lineberger, W. C. *Phys. Rev. A* **1997**, *55*, 2036−2043.
(12) Fox, M.; McIntyre, R.; Hayon, E. *Faraday Discuss. Chem. Soc.* **1977**, *64*, 167−172.
(13) Takahashi, N.; Sakai, K.; Tanida, H.; Watanabe, I. *Chem. Phys. Lett.* **1995**, *246*, 183−186.
(14) Adriaanse, C.; Sulpizi, M.; VandeVondele, J.; Sprik, M. *J. Am. Chem. Soc.* **2009**, *131*, 6046−6047.
(15) Crowell, R. A.; Lian, R.; Shkrob, I. A.; Bartels, D. M.; Chen, X.; Bradforth, S. E. *J. Chem. Phys.* **2004**, *120*, 11712−11725.
(16) Petersen, C.; Thøgersen, J.; Jensen, S. K.; Keiding, S. R. *J. Phys. Chem. A* **2007**, *111*, 11410−11420.
(17) Iglev, H.; Fischer, M. K.; Gliserin, A.; Laubereau, A. *J. Am. Chem. Soc.* **2011**, *133*, 790−795.
(18) Winter, B.; Faubel, M.; Vácha, R.; Jungwirth, P. *Chem. Phys. Lett.* **2009**, *474*, 241−247.
(19) Masamura, M. *J. Chem. Phys.* **2002**, *117*, 5257−5263.
(20) do Couto, P. C.; Cabral, B. J. C. *J. Chem. Phys.* **2007**, *126*, 014509.
(21) do Couto, P. C.; Chipman, D. M. *J. Chem. Phys.* **2012**, *137*, 184301.
(22) Hahn, P. H.; Schmidt, W. G.; Seino, K.; Preuss, M.; Bechstedt, F.; Bernholc, J. *Phys. Rev. Lett.* **2005**, *94*, 037404.
(23) Garbuio, V.; Cascella, M.; Reining, L.; Del Sole, R.; Pulci, O. *Phys. Rev. Lett.* **2006**, *97*, 137402.
(24) Garbuio, V.; Cascella, M.; Pulci, O. *J. Phys.: Condens. Matter* **2009**, *21*, 033101.
(25) Pham, T. A.; Zhang, C.; Schwegler, E.; Galli, G. *Phys. Rev. B* **2014**, *89*, 060202.
(26) Adriaanse, C.; Cheng, J.; Chau, V.; Sulpizi, M.; VandeVondele, J.; Sprik, M. *J. Phys. Chem. Lett.* **2012**, *3*, 3411−3415.
(27) Bernasconi, L. *J. Chem. Phys.* **2010**, *132*, 184513.
(28) Malcioğlu, O. B.; Gebauer, R.; Rocca, D.; Baroni, S. *Comput. Phys. Commun.* **2011**, *182*, 1744−1754.
(29) Ge, X.; Binnie, S. J.; Rocca, D.; Gebauer, R.; Stefano, B. *turboTDDFT 2.0 - Hybrid functionals and new algorithms within time-dependent density-functional perturbation theory*; arXiv:1402.0486 [physics.chem-ph].
(30) Giannozzi, P.; Baroni, S.; Bonini, N.; Calandra, M.; Car, R.; Cavazzoni, C.; Ceresoli, D.; Chiarotti, G. L.; Cococcioni, M.; Dabo, I.; Dal Corso, A.; de Gironcoli, S.; Fabris, S.; Fratesi, G.; Gebauer, R.; Gerstmann, U.; Gougoussis, C.; Kokalj, A.; Lazzeri, M.; Martin-Samos, L.; Marzari, N.; Mauri, F.; Mazzarello, R.; Paolini, S.; Pasquarello, A.; Paulatto, L.; Sbraccia, C.; Scandolo, S.; Sclauzero, G.; Seitsonen, A. P.; Smogunov, A.; Umari, P.; Wentzcovitch, R. M. *J. Phys.: Condens. Matter* **2009**, *21*, 395502.
(31) Becke, A. D. *Phys. Rev. A* **1988**, *38*, 3098−3100.
(32) Lee, C.; Yang, W.; Parr, R. G. *Phys. Rev. B* **1988**, *37*, 785−789.
(33) VandeVondele, J.; Mohamed, F.; Krack, M.; Hutter, J.; Sprik, M.; Parrinello, M. *J. Chem. Phys.* **2005**, *122*, 014515.
(34) Costanzo, F.; Sulpizi, M.; Valle, R. G. D.; Sprik, M. *J. Chem. Phys.* **2011**, *134*, 244508.
(35) Perdew, J. P.; Burke, K.; Ernzerhof, M. *Phys. Rev. Lett.* **1996**, *77*, 3865−3868.
(36) Perdew, J. P.; Burke, K.; Ernzerhof, M. *Phys. Rev. Lett.* **1997**, *78*, 1396−1396.
(37) Heyd, J.; Scuseria, G. E.; Ernzerhof, M. *J. Chem. Phys.* **2003**, *118*, 8207−8215.
(38) Heyd, J.; Scuseria, G. E.; Ernzerhof, M. *J. Chem. Phys.* **2006**, 124.
(39) Winter, B.; Faubel, M.; Hertel, I. V.; Pettenkofer, C.; Bradforth, S. E.; Jagoda-Cwiklik, B.; Cwiklik, L.; Jungwirth, P. *J. Am. Chem. Soc.* **2006**, *128*, 3864−3865.
(40) Bernasconi, L.; Sprik, M.; Hutter, J. *J. Chem. Phys.* **2003**, *119*, 12417−12431.
(41) Bernasconi, L.; Sprik, M.; Hutter, J. *Chem. Phys. Lett.* **2004**, *394*, 141−146.